Pore geometry and isosteric heat : an analysis for the carbon dioxyde adsorption on activated carbon.

Dominique Levesque, Farida Darkrim Lamari

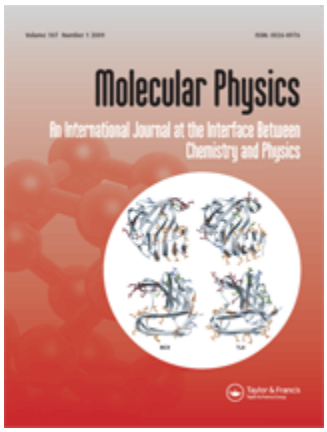

Pore geometry and isosteric heat : an analysis for the carbon dioxyde adsorption on activated carbon.

Journal:	*Molecular Physics*
Manuscript ID:	TMPH-2008-0446.R1
Manuscript Type:	Special Issue Paper - Dr. Jean-Jacques Weis
Date Submitted by the Author:	16-Mar-2009
Complete List of Authors:	Levesque, Dominique; Université de Paris-Sud XI, Laboratoire de Physique Théorique Darkrim Lamari, Farida; University Paris 13, Institut Galilee
Keywords:	adsorption, isosteric heat
Note: The following files were submitted by the author for peer review, but cannot be converted to PDF. You must view these files (e.g. movies) online.	
TMPH-2008-0446_R1.tex	

Molecular Physics
Vol. 00, No. 00, Month 200x, 1–8

RESEARCH ARTICLE

Pore geometry and isosteric heat : an analysis for the carbon dioxyde adsorption on activated carbon

Dominique Levesque [a] * and Farida Darkrim Lamari[b]

[a] *LPT UMR CNRS 8627 Université Paris XI Bâtiment 210, 91405 Orsay, France*
[b]*LIMHP Université Paris XIII, CNRS UPR 1311, Institut Gallilée, 93430 Villetaneuse, France*

(*Received 00 Month 200x; final version received 00 Month 200x*)

The isosteric heat of the carbon dioxide adsorption on activated carbon is determined by grand canonical Monte Carlo simulations. The results, obtained at room temperature and low pressures for an adorbent model with a slit type porosity, show that the isosteric heat depends strongly on the slit width. The maximun of the isosteric heat is reached for a pore with a width such as cooperative effects between the adsorbed molecules enhance the adsorption. The possibility to estimate the isosteric heat of a macroscopic sample, from adsorption isotherms computed for a distribution of slit pores with given sizes, is discussed.

Introduction

The isosteric heat is a very important characteristic of the adsorption phenomena. Its value is relevant, in particular for the first stages of the adsorption process, since the released heat increases the delay to achieve an equilibrium state between the adsorbed phase and bulk phase in contact with the porous material. In addition, a large isosteric heat induced by a strong interaction between adsorbed molecules and adsorbing surface can slow the gas desorption. Hence, the determination of the isosteric heat has been studied in many theoretical and experimental works for various adsorbent materials (activated carbons, zeolites, silicalites, ...) and adsorbed gases (cf., for example, some recent publications [1–11]). For a theoretical computation of the isosteric heat, the adsorbents divide into two main categories. The porous materials, as the zeolites, with a crystalline structure have identical pores at the microscopic scale. For these adsorbents, to estimate the isosteric heat for one or few unit cells of the porous crystal is sufficient to have a reliable value of that of the bulk material. For the porous materials with complex pore networks, as the activated carbons, the whole isosteric heat of a material sample depends on the isosteric heat value associated to each pore type. So, the theoretical calculation of the isosteric heat requires to known the pore size distribution which defines the material porosity and the set of isosteric heats which vary with the pore properties.

The changes of the isosteric heat value with the pore size and shape have been studied mainly by numerical simulations or theoretical methods, as the density functional theory [12–14]. Using a theoretical approximate scheme, Schindler and LeVan [15] have shown that the isosteric heat of simple gases Ar, N_2, CO_2 or CH_4 adsorbed in graphite slit pores has a maximal value when the slit width, defined

*Corresponding author. Email: dominique.levesque@th.u-psud.fr

ISSN: 0040-5167 print/ISSN 1754-2278 online

DOI: 10.1080/0040516YYxxxxxxxx
http://www.informaworld.com

as the distance between the carbon atoms located inside the slit walls, is of the order of ~ 0.7 nm. In this work, we present the results of a similar calculation for CO_2 performed by using grand canonical Monte-Carlo (GCMC) simulations which allow to take into account the contribution to the adsorption process from important cooperative effects between the CO_2 adsorbed molecules. These effects, combined with the modification of the molecule-adsorbent interaction when the slit width varies, lead to large differences between the pore isosteric heats. Such differences imply that an adequate method must be used to determine the isosteric heat of activated carbon samples with various pore size distributions from those computed for a set of slit pores with a given width [16].

In the first part of this work, is described the model considered for studying the CO_2 adsorption in graphitic slit pores. The results of GCMC simulations of this process are presented in the second section. The third section is devoted to the discussion of the simulation results and to their possible use for a comparison with experimental data.

Model Description

The CO_2 molecule is modeled as a linear rigid molecule of length equal to 0.232 nm and its molecular interactions are described by Lennard-Jones (LJ) pair potential centers of generic equation $v_{\rm LJ}(r) = 4\epsilon[(\sigma/r)^{12} - (\sigma/r)^6]$. Two of these potentials correspond to oxygen atoms and are located to the molecule ends. The third potential corresponds to the carbon atom and is located to the middle of the molecule. The LJ parameters of oxygen and carbon potentials are $\epsilon_0 = 79.0$ K, $\sigma_0 = 0.305$ nm, and $\epsilon_C = 27.0$ K, $\sigma_C = 0.28$ nm, respectively. In addition, the linear quadrupole of the CO_2 molecule is described by a neutral distribution of three charges located at the LJ center positions. The charges on the O atom positions are equal to -0.35 e, that on the C atom position is 0.70 e (e electronic charge). This model of CO_2 interaction has been tested sucessfully in the literature [17, 18]. The interaction of the carbon atom in a graphite plane is a LJ potential with parameters $\epsilon_G = 28.0$ K and $\sigma_G = 0.340$ nm. The cross-interaction between CO_2 molecules and between CO_2 molecules and carbon atoms of the pore walls are derived by using the Berthelot's rule, expressed by the relations : $\sigma_{\alpha\,\beta} = 0.5\,(\sigma_\alpha + \sigma_\beta)$ and $\epsilon_{\alpha\,\beta} = \sqrt{\epsilon_\alpha \epsilon_\beta}$ where the indices α and β refer to the indices O, C or G of the LJ parameters of a CO_2 molecule and carbon atom. Such an effective potential for the graphite carbon atoms and the rule used to compute the gas-graphite interactions have been justified by many studies, cf., for instance, the work on the graphite cohesion energy [19], the text-book [20] and the recent comparison with ab-initio calculations [21].

The activated carbon model supposes that the material pores are mainly slits with different widths [22]. The pore walls are made from a stack of three graphite basal planes. Inside the stack, the distance between the planes is equal to 0.34 nm. The slit width h is defined as the distance between carbon atoms located in the external planes of pore opposite walls. With these characteristics, the specific surface of the material model is ~ 1030 m^2/gr.

The potential energy of one single CO_2 molecule inside slit pores of the model material is presented in Fig. 1. The energy potential varies strongly with increasing h and molecule orientation. Fig. 1(a) gives the potential energy for a molecule the axis of which is parallel to the pore walls and Fig. 1(b) for a molecule the axis of which is perpendicular. For a given h value, the potential energy of a molecule parallel to the walls is larger than that of a molecule perpendicular to the walls. For $h \leq 0.5$ nm, the simulations show that in the considered range of pressure at room

temperature no CO_2 molecule can be adsorbed in pores with such a width. For 0.6 nm $\leq h \leq$ 0.8 nm, the potential energy for a molecule with its axis perpendicular to the walls is strongly positive and is not plotted. For $h \geq$ 0.8 nm, for both molecular axis orientations, the potential has two minima which are located in the wall vicinity.

Simulation Results

The GCMC simulations are realized following the procedure described in the litterature [23–25]. The GCMC code developed by us and used in previous works, for instance [26], implement the Metropolis algorithm adapted to the configuration sampling of a GC ensemble in a standard way. Specifically, an initial configuration of adsorbed molecules in the volume filled with the adsorbent is generated. From this initial configuration the new configurations are sampled by iteratively attempting to insert a new molecule at random in the volume, to delete or to displace randomly one of molecules present in the volume chosen at random. These changes are accepted or refused accordingly to the GC Boltzmann weight ratio of the previous and trial configurations. The set of generated configurations allows to compute the average values of quantities as the energy and molecule number.

The simulation cell is parallelepipedic with periodic boundary conditions in the x, y and z directions. It contains two stacks of graphite basal planes. These stacks, constituted of three planes, are positioned perpendicularly to the z axis. The x and y dimensions of planes are chosen identical to those of the simulation cell in order that the hexagonal arrangement of C atoms and the cell boundary conditions are compatible. The two stacks form the pore walls and are placed in such a way to define two slits wih same width h taking into account the boundary conditions. The cell size is equal to 8.116 and 4.257 nm in the x and y directions, respectively, and, in the z direction, it varies between 2.537 and 6.339 nm when h varies between 0.6 nm and 2.5 nm. The cell contains 7920 C atoms. For an efficient computation of the molecule energy, a cell linked list algorithm [24] is used by partitioning the simulation volume in parallelepipedic sub-volumes with edge equal to or larger than the interaction range.

For a given pressure P, temperature T and chemical potential μ, the total adsorption m_a, expressed in mol per gram of adsorbent, is given by

$$m_a = \frac{< N_a >}{N_C M_C} \tag{1}$$

where $< N_a >= \bar{N}_a$ is the average value of the adsorbed molecule number. N_C is the number of C atoms in the simulation cell and M_C the carbon molar mass. The excess adsorption m_e, obtained in removing the contribution of compression effects to m_a, is defined by $m_e = m_a - \rho_b V_f$. ρ_b is the density of the gas in the bulk phase in mmol per volume unit and V_f the free volume accessible to the adsorbed gas per gram of adsorbent. The V_f values have been computed from the amount of Helium adsorbed m_a^{He} in the slit pores by GCMC simulation at 653 K and 0.1 MPa. In agreement with the experimental Helium displacement method [27], V_f is given by $V_f = m_a^{He}/\rho_b^{He}$ where ρ_b^{He} is the Helium bulk density at 653 K and 0.1 MPa. The bulk pressure and density associated to the μ value used in a simulation run at given T were determined from GCMC simulations performed with a simulation cell containing no adsorbent.

The isosteric heat q_i, following the definition quoted from refs. [23, 28], is "the differential entropy change in a reversible process where fluid is tranferred from

the porous material at fixed volume and temperature to the bulk phase at fixed temperature and bulk pressure". It is given by

$$q_i = T\Big\{\Big(\frac{\partial S_b}{\partial \bar{N}_b}\Big)_{T,P} - \Big(\frac{\partial S_a}{\partial \bar{N}_a}\Big)_{T,V_f}\Big\} \tag{2}$$

where S_b and S_a are the entropies and $\bar{N}_b$ and $\bar{N}_a$ the molecule numbers of the bulk and adsorbed phases. This expression can be rewritten as

$$q_i = H_b - \Big(\frac{\partial \bar{U}_a}{\partial \bar{N}_a}\Big)_{T,V_f} \tag{3}$$

where H_b is the enthalpy per molecule of the bulk phase and $\bar{U}_a$ the energy of the adsorbed phase. When $\partial \bar{U}_a/\partial \bar{N}_a$ is expressed in terms of fluctuations of $\bar{U}_a$ and $\bar{N}_a$ in the GC ensemble, q_i writes

$$q_i = H_b - \frac{< U_a N_a > - < U_a >< N_a >}{< N_a^2 > - < N_a >^2} \ , \tag{4}$$

a formula adapted to the q_i computation by GCMC simulations. Taking into account the expression of H_b in terms of the pressure and energy at a fixed temperature, we can write:

$$q_i = P/\rho_b + U_b^c + U_b^i - U_a^c - \frac{< U_a^i N_a > - < U_a^i >< N_a >}{< N_a^2 > - < N_a >^2} \tag{5}$$

where U_b^c and U_a^c, the average kinetic energies per molecule of the bulk and adsorbed phases, are equal obviously to $5k_BT/2$ for CO_2 (k_B Boltzmann constant). U_b^i is the internal energy per molecule of the bulk phase and U_a^i that of the adsorbed phase. The hypothesis that the bulk phase is a perfect gas, leads to the approximate formula often used in the literature :

$$q_i = k_BT - \frac{< U_a^i N_a > - < U_a^i >< N_a >}{< N_a^2 > - < N_a >^2} \, . \tag{6}$$

m_a and q_i have been estimated from GCMC runs comprising, at least, 12×10^6 MC steps to achieve the equilibium state of adsorbed phases followed by 48×10^6 MC steps to compute the average quantities. These numbers of MC steps were sufficient for slit pores with $h \geq 0.9$ nm to determine m_a and q_i with a statistical uncertainty ∼1-2%. For the pores with $h \leq 0.8$ nm, the statistical error on m_a is similar but the values of $< N_a >^2$ and $< N_a^2 >$ being close, $< N^2 > - < N >^2$ is difficult to estimate accurately and the uncertainty on the q_i values is of the order of $\sim 5\%$ for $h = 0.6$ and 0.7 nm and $\sim 10\%$ for $h = 0.8$ nm.

The excess adsorption isotherms and q_i values at $T = 293$ K between 0.01 and 0.20 MPa for slit pores with increasing widths are presented in Fig. 2 and 3. For pores with $h \geq 0.9$ nm, the excess adsorption m_e varies monotically and this variation is almost proportional to that of the pressure. By contrast, for $h = 0.8$ nm, m_e remains quasi constant between 0.02 and 0.2 MPa, a behavior which results from the tight stack of the adsorbed molecules for this pore size. A snapshot of the molecule arrangement is given in Fig. 5 ; it shows that molecules are in average slightly tilted with respect to the orientation where they would be perpendicular to the the pore walls. In such configurations, where the contribution to U_a and q_i from the molecule-molecule interaction U_a^m and molecule-adsorbent interaction

U_a^G are almost equal, the cooperative effects between molecules have an important role in the adsorption process. For $h = 0.7$ nm, these effects remain important since $U_a^G/5 < U_a^m < U_a^G/2$ in the pressure range 0.01-0.2 MPa. At $h = 0.6$ nm, the confinement involves that the molecules are parallel to the pore walls and from the disorder of the bidimensional molecular arrangement inside the slit (cf. snapshot in Fig. 5), it results that U_a^m is of the order of $U_a^G/15$ at 0.01 MPa and $U_a^G/7$ at 0.2 MPa. For the size $h = 2.5$ nm, U_a^m varies from ~ 0.0 at 0.01 MPa to $U_a^G/15$ at 0.2 MPa.

These data and the modification of the molecule-adsorbent interactions when h increases (cf. Fig. 1) help to the interpretation of the variation of q_i with those of P and h. When the interaction between molecules is negligible or weak in the adsorbed phase, to a good approximation q_i has a value determined by the only interaction of one molecule with the adsorbent surface implying that $< U_a^i N_a > - < U_a^i >< N_a >$ is almost proportional to $< N_a^2 > - < N_a >^2$. In this case and when, for h sufficiently large, the molecule-adsorbent interaction has no more variation with h, q_i depends little on P and h, as it is found by simulation for the adsorption in pores with $h > 1.2$ nm. For h between 0.9 nm and 1.2 nm, to the strong increase of m_e with the pressure corresponds an increase of the U_a^m contribution to U_a from 2% up to 30% while the U_a^G contribution per molecule remains constant. As a consequence of the variation of U_a^m and $< N_a^2 > - < N_a >^2$ when the molecule density in the pores increases, q_i varies by 30 % in the considered pressure range. In the narrow pores, in particular for 0.8 nm, m_e is close to m_a and varies only by 10-20% between 0.01 and 0.2 MPa. Due to the packing of the molecules $< N_a^2 > - < N_a >^2$, which has a value much smaller than its perfect gas value equal to $< N >$, U_a and $< U_a N_a > - < U_a N_a >$ vary little and q_i remains quasi constant between 0.01 and 0.2 MPa.

Similarly to the results obtained in [15], m_e and q_i present a maximum for a pore with a width of $h \simeq 0.8$ nm. But the maximum values of q_i are larger by a factor of ~ 2 as a consequence of the strong contribution of the intermolecular interactions in the adsorbed phase and m_e and q_i have almost achieved at 0.1 MPa their maximal values.

Discussions and Conclusions

For the considered temperature and pressure domain, the strong variations of m_e and q_i with the pore size give a typical example of the difficulty to compare the simulation results with experimental data for CO_2 adsorbed on activated carbons. Only, in the cases where the material porosity is very homogeneous or corresponds to slit widths larger than 1.6 nm, such a comparison can be easily performed, since all pores contribute almost similarly to the excess adsorption. When the activated carbon pore network comprises slits with widths smaller than 1.0 nm, the excess adsorption of the material need to be estimated from an average where the excess adsorptions computed for each slit type is weighted in agreement with the pore size distibution [6, 16, 29]. Supposing that the pores differ only in width, m_e the excess adsorption per gram of adsorbent is given by

$$m_e = \int m_a^h \, v(h) dh - \rho_b V_f \tag{7}$$

where m_a^h is the total amount of adsorbed gas in a slit pore with width h and free volume unity. $v(h)dh$ ($V_f = \int v(h)dh$) is the contribution to V_f from pores with width between h and $h + dh$.

For the q_i computation of activated carbons, Birkett and Do [16] have shown that a formula, similar to Eq. 7, expressing q_i as a weigthed average on the isosteric heats q_i^h of the slits with width h is incorrect and should be replaced by

$$q_i = H_b + \frac{\int q(h)_i \left(\partial \bar{N}_a^h / \partial \bar{P}\right)_{T,V_h} v(h) dh}{\left(\partial \bar{N}_a / \partial \bar{P}\right)_{T,V_f}} \tag{8}$$

where $\bar{N}_a^h$ is the molecule number adsorbed in a slit with a width h and free volume unity and $q(h)_i = q_i^h - H_b$. In practice the use of Eq. 7 and 8 with simulation results, supposes that the pore size distribution $v(h)$ is experimentally known and partial derivatives are estimated from discrete approximations.

Experimental estimates of q_i are often obtained from adsorption isotherms determined at close temperature intervals by using the formula [28],

$$q_i = \frac{T}{\rho_b} \left[\frac{dP}{dT}\right]_{eq,m_a} \tag{9}$$

where the subscript eq, m_a indicates that the pressure derivative with respect to temperature is computed at equilibrium between bulk and adsorbed phases and constant value of m_a. The possibility that a correct estimate of q_i for adsorbents, such as active carbons, can be obtained from Eq. 9 depends on its compatibility with Eq. 8 which has to be established and, obviously on its validity when it is used for a single pore with a given width. By computing adsorption isotherms at temperatures 298 K and 288 K, $[dP/dT]_{eq,m_a}$ can be calculated at 293 K from

$$\left[\frac{dP}{dT}\right]_{eq,m_a} = \frac{P(T+dT, m_a) - P(T-dT, m_a)}{2dT} \tag{10}$$

where $P(T+dT, m_a)$ and $P(T-dT, m_a)$ are the pressures on isotherms at temperatures $T+dT$ and $T-dT$ where the total adsorption is equal to the value m_a obtained at a given pressure P on the isotherm at temperature T. Such a verification of the agreement between the Eqs. 4 and 9 is successful when the slit pores have widths $h \geq 1.6$ mn. For instance, for $h = 2.5$ nm from Eq. 4, q_i is equal to 14.1 and 14.7 kj/mol at $P = 0.02$ and 0.1 MPa, respectively, and, from Eq. 9, equal to 14.5 and 15.2 kj/mol. The differences of few percents between the estimates of q_i are compatible with the statistical error on simulations results and uncertainty which results from the discrete approximation of the pressure derivative. For $h \leq 1.2$ nm the discrepancy between the two estimates of q_i increases when h decreases and at $h = 0.6$ nm and $P = 0.02$ and 0.10 MPa, q_i values obtained from Eq. 4 are, respectively equal to 33.1 and 37.3 kj/mol and, from Eq. 9, equal to 37.1 and 46.7 kj/mol. The explanation of such differences is the large numerical error on the dP/dT estimate from isotherms at temperatures differing by 10 K in the pressure domain where, m_a varies quite slowly. In fact, a precise estimate of $(dP/dT)_{eq,m_a}$ for $h = 0.6$ nm at 293 K, can be only obtained from very accurate computations of the adsorption isotherms at 295 and 291 K. Using the results of such computations, Eq. 10 give, for $h = 0.6$, q_i equal to 33.3 and 37.7 kj/mol at $P = 0.02$ and 0.10 in close agreement with the simulation data obtained from Eq. 4. So, it seems possible to determine q_i from Eq. 9 for the mesopores $h \simeq 1.5 - 2.0$ nm and micropores $h \leq 0.9$ nm when, in the latter case, adsorption isoterms, differing in temperature only by few degrees are determined with an accuracy of $\simeq 0.2\%$ in the domain of pressures where m_a is almost constant.

In summary, our calculations of the CO_2 adsorption and isosteric heat in graphitic

slit pores of various widths are compatible with experiments, (cf., for instance, [8]) and show that, at room temperature and low pressures, an unambiguous comparison between simulation data and adsorption experiments on activated carbon seems only possible when the pore size distribution of the material is known or if, in the pore network, the pores have mainly a width larger than 1.5 nm. They also show that in narrow pores ($h \simeq 0.8$ nm), the excess weight percent is of the order of 20 %, a value obviously favorable for the CO_2 capture.

References

[1] D.D. Do, D. Nicholson and H.D. Do, J. Colloid Interface Sci. **324**, 15 (2008).
[2] D.D. Do, D. Nicholson and H.D. Do, J. Colloid Interface Sci. **325**, 7 (2008).
[3] D.D. Do and H.D. Do, J. Phys. Chem. B **110**, 17531 (2006).
[4] G.R. Birkett and D.D. Do, Adsorption **13**, 407 (2007).
[5] S.K. Jain, K.E. Gubbins, R.J.-M. Pellenq and J.P. Pikunic, Carbon **44**, 2445 (2006).
[6] D. Nicholson, Langmuir **15**, 2508 (1999).
[7] R. Babarao, Z. Hu, J. Jiang, S. Chempath and S.I. Sandler, Langmuir **23**, 659 (2007).
[8] B. Guo, L. Chang and K. J. Xie, Nat. Gas Chem. **15**, 223 (2006).
[9] S. Himeno, T. Komatsu and S. J. Fujita, Chem. Eng. Data **50**, 369 (2005).
[10] M. Bienfait, P. Zeppenfeld, N. Dupont-Pavlovsky, M. Muris, M.R. Johnson, T. Wilson, M. DePies and O.E. Vilches, Phys. Rev. B **70**, 035410 (2004).
[11] J.-S. Lee, J.-H. Kim, J.-T. Kim, J.-K. Suh, J.-M. Lee and C.-H. Lee, J. Chem. Eng. Data **47**, 1237 (2002).
[12] E.A. Ustinov, D.D. Do and V.B. Fenelonov, Carbon **44**, 653 (2006).
[13] H. Pan, J. A. Ritter and P. B. Balbuena, Langmuir **14**, 6323 (1998).
[14] P.B. Balbuena and K.E. Gubbins, Langmuir **9**, 1801 (1993).
[15] B.J. Schindler and M.D. LeVan, Carbon **46**, 644 (2008).
[16] G. Birkett, D.D. Do, Langmuir. **22**, 9976 (2006).
[17] J.M. Stubbs and J.I. Siepmann, J. Chem. Phys. **121**, 1525 (2004).
[18] J.G. Harris and K.H. Yung, J. Chem. Phys. **99**, 12021 (1995).
[19] L.A Girifalco and R.A. Lad, J. Chem. Phys. **25**, 693 (1956).
[20] W.A. Steele, *The interaction of gases with solid surfaces*, (Pergamon Press, Oxford, 1974).
[21] D.Y. Sun, J.W. Liu, X.G. Gong and Zhi-Feng Liu, Phys. Rev. B **75**, 075424 (2007).
[22] J.W. Patrick, editor, *Porosity in Carbons* (Edward Arnold, London, 1995).
[23] D. Nicholson and N.G. Parsonage, *Computer Simulation and the Statistical Mechanics of Adsorption*, (Academic Press, London, 1982).
[24] M.P. Allen and D.J. Tildesley, *Computer Simulation of Liquids*, (Oxford University Press, New York, 1990).
[25] D. Frenkel and B. Smit, *Understanding Molecular Simulation*, (Academic Press, London, 2002).
[26] B. Weinberger, F. Darkrim-Lamari, and D. Levesque, J. Chem. Phys. **124**, 234712 (2006).
[27] P. Malbrunot, D. Vidal, J. Vermesse, R. Chahine and T.K. Bose, Langmuir **13**, 539 (1997).
[28] T. Vuong and P.A. Monson, Langmuir **12**, 5425 (1996).
[29] Y. He and N.A. Seaton **21**, 8297 (2005).

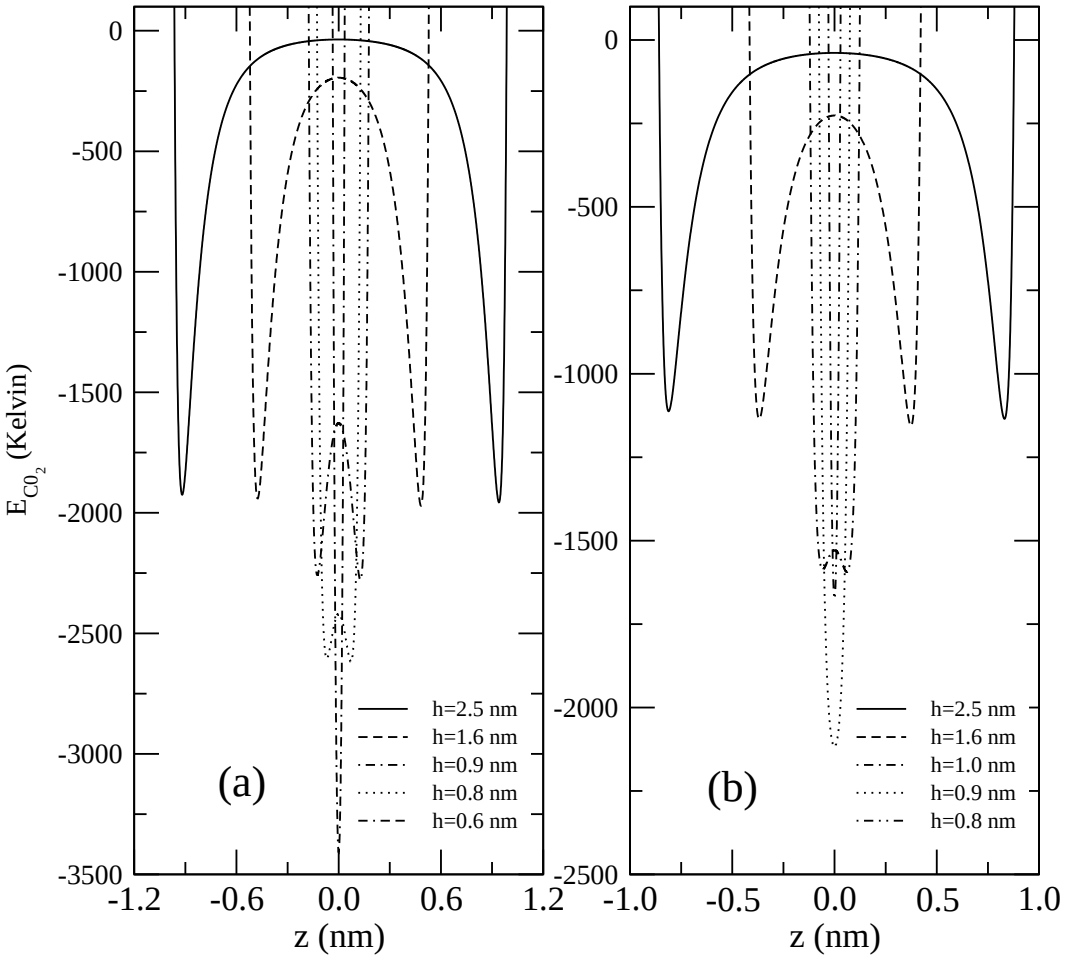

Figure 1. Potential energy (Kelvin degree) of one CO_2 molecule in graphitic slit pores with widths increasing from 0.6 nm to 2.5 nm. Fig. 1(a) : axis of the molecule parallel to the pore walls, Fig. 1 (b) : axis of the molecule perpendicular to the pore walls. The middle of the slit is the coordinate origin of the z axis.

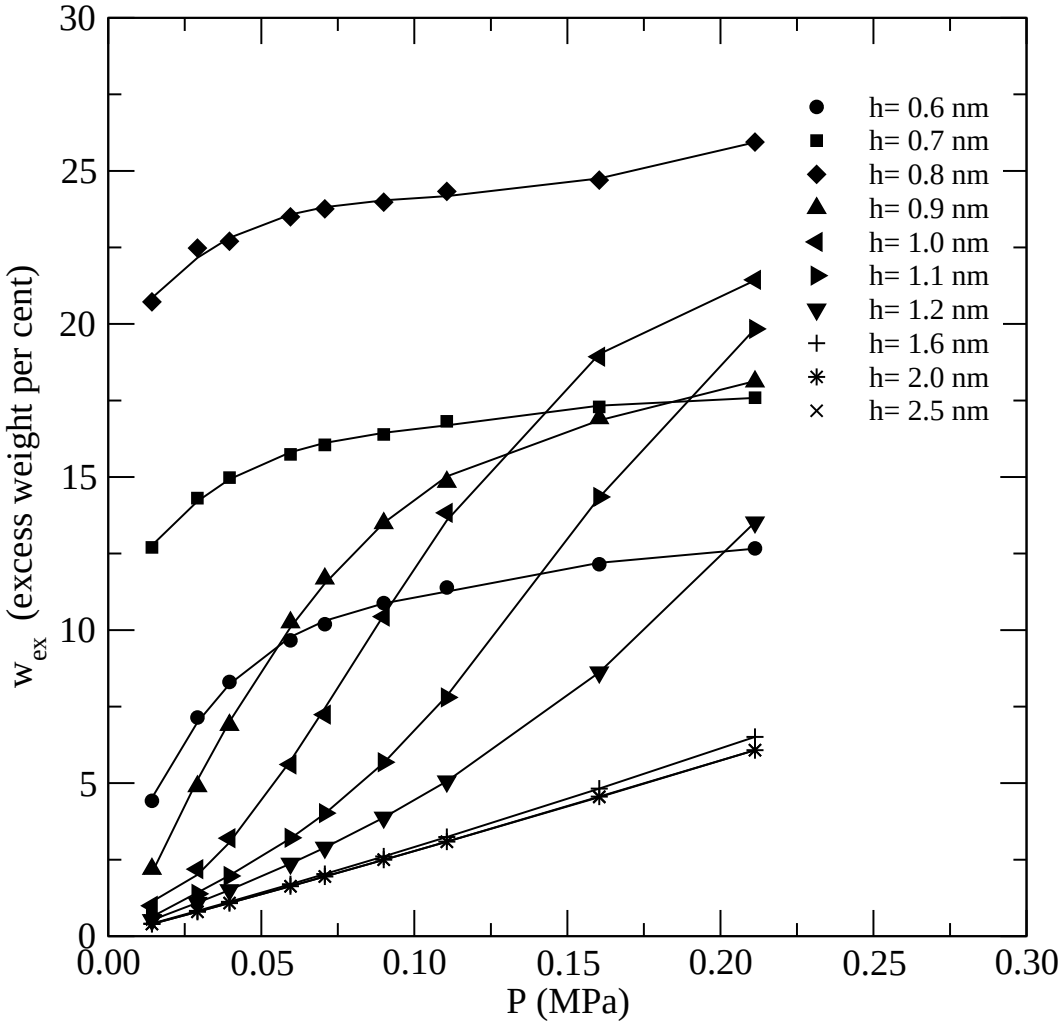

Figure 2. Excess adsorption ($w_{ex} = 100\ m_e\, M_{CO_2}$, M_{CO_2} molar mass of CO_2) for graphitic slit pores with widths increasing from 0.6 nm to 2.5 nm at $T = 293$ K.

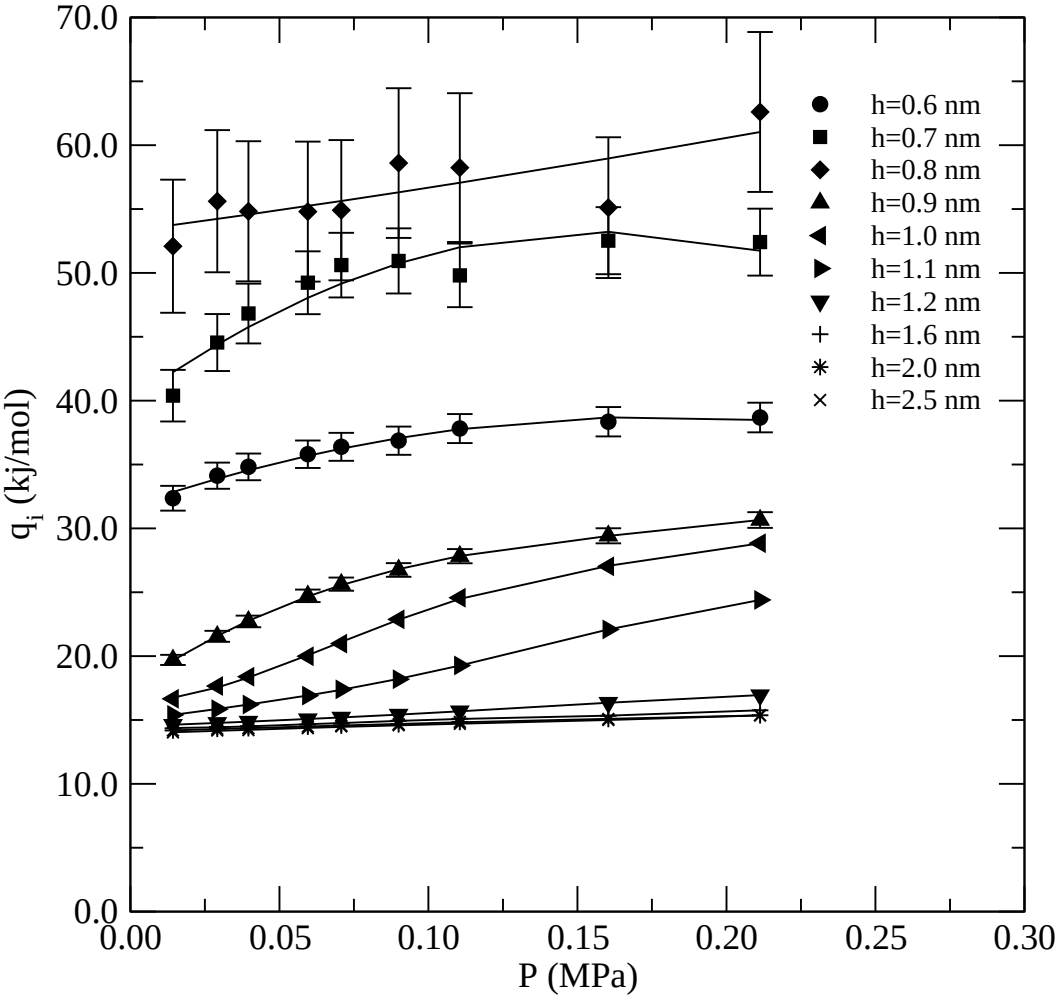

Figure 3. Isosteric heat (kj/mol) for graphitic slit pores with widths increasing from 0.6 nm to 2.5 nm at $T = 293$ K.

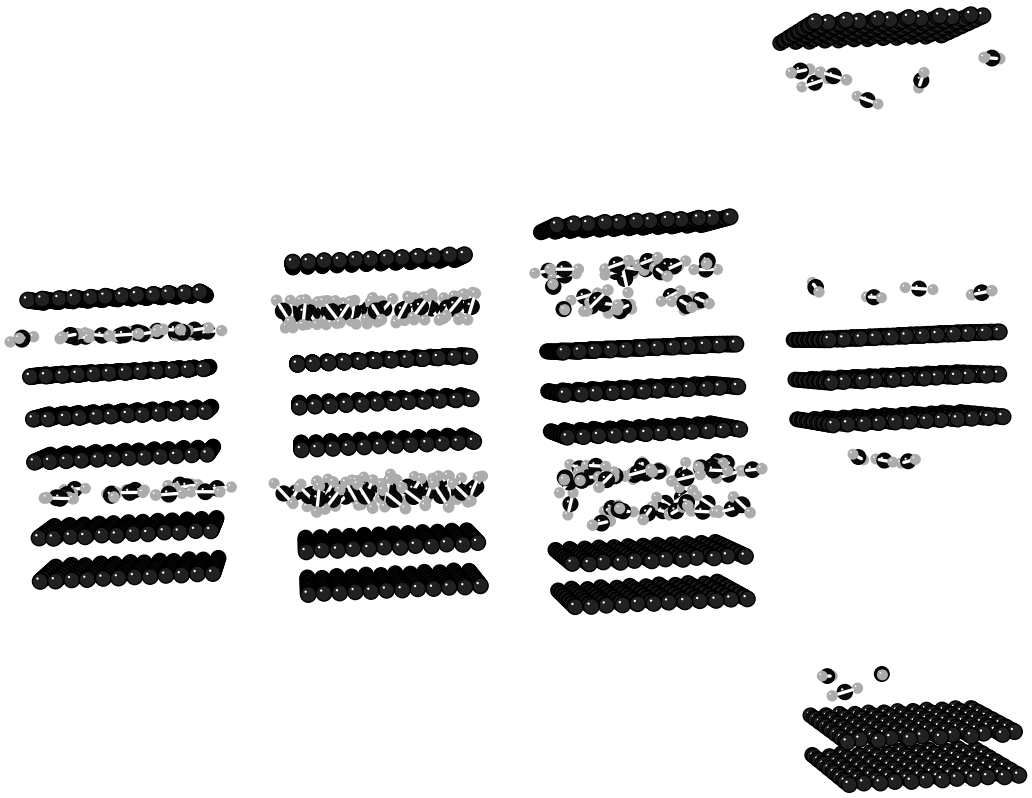

Figure 4. From left to right, snapshots of the local arrangements of CO_2 molecules in slits of width equal to 0.6 nm, 0.8 nm, 1.0 nm and 2.5 nm at $P = 0.1$ MPa and $T = 293$ K.

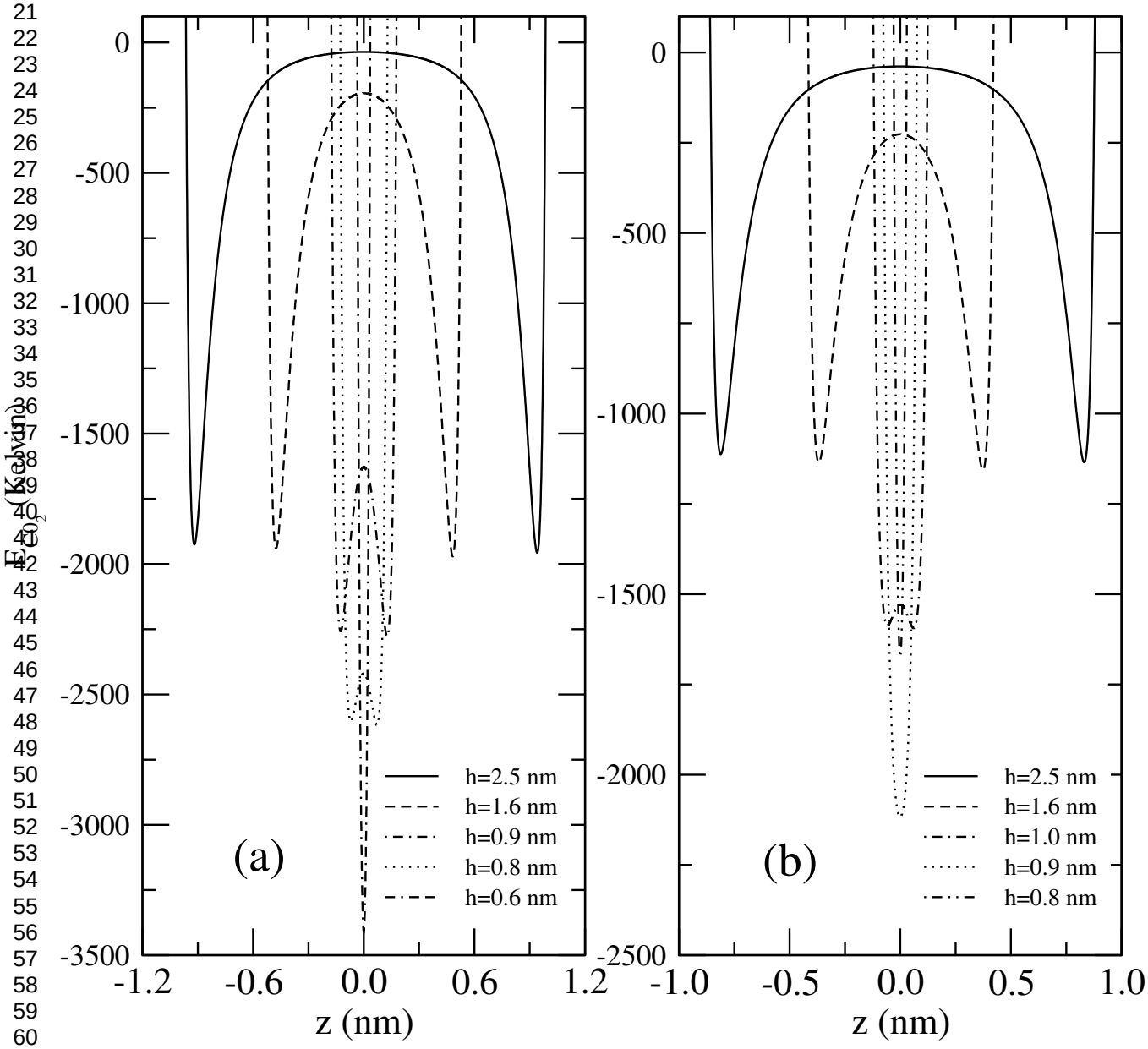
0
-500
-1000
-1500
-2000
-2500
-3000
-3500
-1.2
-0.6
0.0
0.6
1.2
z (nm)
E_{CO_2} (Kelvin)
h=2.5 nm
h=1.6 nm
h=0.9 nm
h=0.8 nm
h=0.6 nm
(a)
0
-500
-1000
-1500
-2000
-2500
-1.0
-0.5
0.0
0.5
1.0
z (nm)
h=2.5 nm
h=1.6 nm
h=1.0 nm
h=0.9 nm
h=0.8 nm
(b)

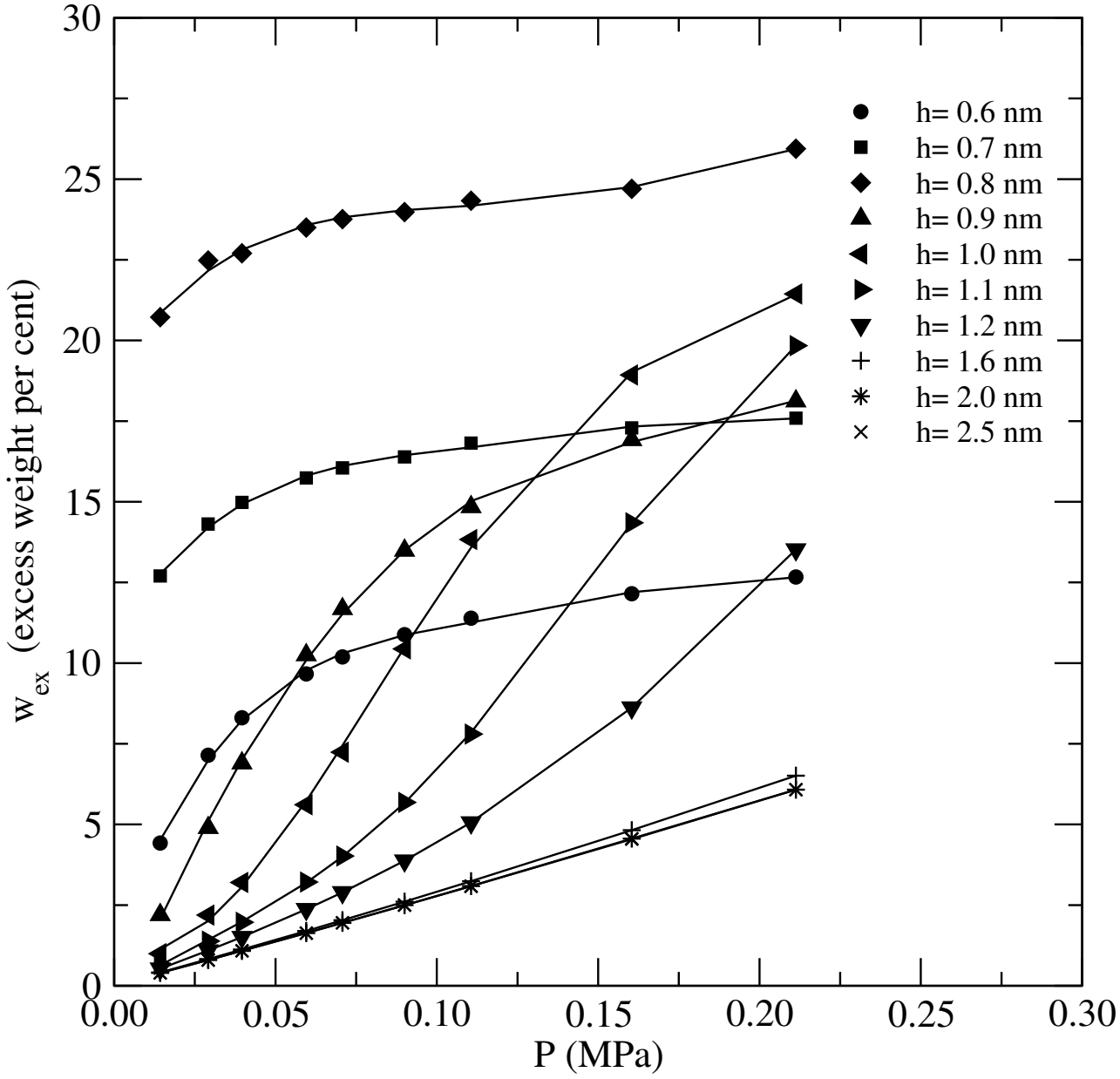
30
25
20
15
10
5
0
0.00
0.05
0.10
0.15
0.20
0.25
0.30
P (MPa)
w_{ex} (excess weight per cent)
h= 0.6 nm
h= 0.7 nm
h= 0.8 nm
h= 0.9 nm
h= 1.0 nm
h= 1.1 nm
h= 1.2 nm
h= 1.6 nm
h= 2.0 nm
h= 2.5 nm

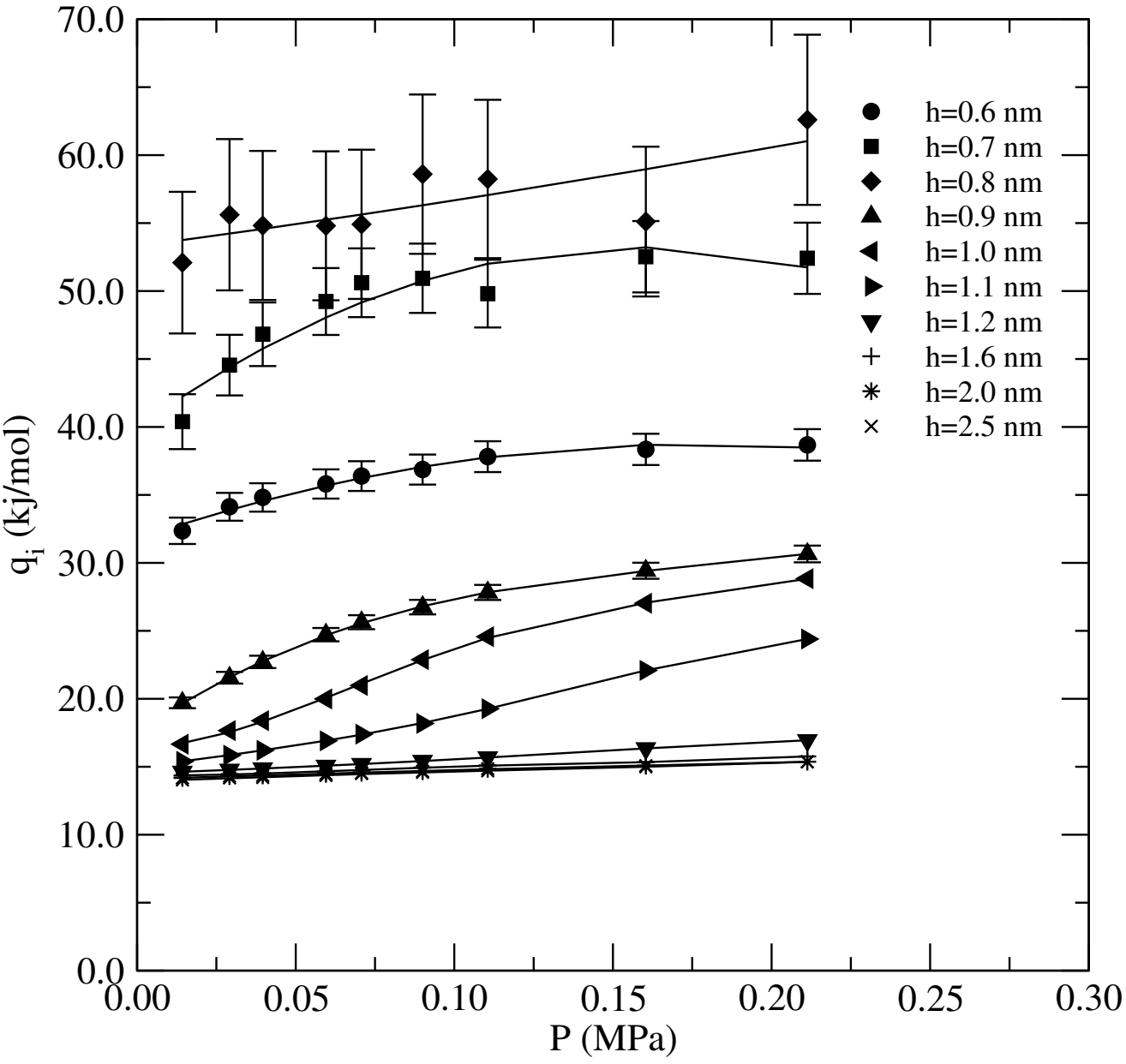
70.0
60.0
50.0
40.0
30.0
20.0
10.0
0.0
0.00
0.05
0.10
0.15
0.20
0.25
0.30
P (MPa)
q_i (kj/mol)
h=0.6 nm
h=0.7 nm
h=0.8 nm
h=0.9 nm
h=1.0 nm
h=1.1 nm
h=1.2 nm
h=1.6 nm
h=2.0 nm
h=2.5 nm